Unusual magnetic ordering transitions in nanoscale biphasic LuFeO₃: Role of ortho-hexa phase ratio and local structure

Smita Chaturvedi, [1,2,9*] *Priyank Shyam,* [3] *Mandar M. Shirolkar,* [4,5,] *Swathi Krishna* [1,2], *Bhavesh Sinha,* [6] *Wolfgang Caliebe,* [7] *Aleksandr Kalinko,* [8] *Gopalan Srinivasan* [9] *and Satishchandra Ogale* [,2,10*]

[1]*Interdisciplinary School of Science, Savitribai Phule Pune University, Ganeshkhind , Pune - 411007, India*

[2]*Centre for Energy Science, Indian Institute of Science Education and Research, Pune - 411008, India*

[3]*Interdisciplinary Nanoscience Center, Aarhus University, Gustav Wieds Vej 14, Aarhus, Denmark*

[4]*Department of Physics, Tamkang University, Tamsui 251, Taiwan*

[5] *Symbiosis Centre for Nanoscience and Nanotechnology (SCNN), Symbiosis International (Deemed University), Lavale, Pune, 412115 India*

[6]*National Center for Nanosciences and Nantechnology, University of Mumbai,Kalina, Santakruz(E) Mumbai-400098*

[7] *Deutsches Elektronen-Synchrotron, Photon Science, Notkestr, 85, 22607 Hamburg, Germany.*

[8]*Paderborn University, Warburger Strasse 100, 33098 Paderborn, Germany*

[9]*Physics Department, Oakland University, Rochester, Michigan 48309-4401*

[10] *Research Institute for Sustainable Energy, TCG-Centres for Research and Education in Science and Technology, Sector V, Salt Lake, Kolkata-700091, India*

Electronic Supplementary Information

Experimental details:

Synthesis:

LFO NP were synthesized using a similar sol-gel route combined with post-synthesis annealing.[1] For the synthesis of LFO-NF electrospinning technique was used. : A solution of 1.39 g of PVP and 6 mL of ethanol kept for stirring for 12 hours. Then the solution of 2: 1.9268 gm of $Fe(NO_3)_3 \cdot 9H_2O$, 1.725 gm of $Lu(NO_3)_3 \cdot xH_2O$ with 5 mL ethanol and 5 mL water was prepared. The two solutions thus made were mixed; stirred for 1 h. and then the final solution was transferred to a syringe for electrospinning. Electrospinning was performed at 22 kV and flow rate was maintained to 0.2mL/h The collected fiber was dried at 373 K and kept for annealing at 1123 K. The NP and NF were annealed upto the temperature just below the

temperature of forming the pure orthorhombic phase, for the reason to assess the stability of hexagonal phase in different morphologies.

Characterization

The room-temperature X-ray diffraction (XRD) of the powder samples was performed using a Bruker AXS D8 ADVANCE diffractometer. The lattice parameters were obtained by Rietveld refinement using the software FULLPROF SUITE. The refinement of XRD data established that Nanoparticles have 75 % orthorhombic phase and 25 %-hexagonal phase, while nanofibers have 23 % orthorhombic phase and 77%-hexagonal phase.

Transmission electron microscopy (TEM), high-resolution TEM (HRTEM) and EDS mapping in STEM mode of both the synthesized powder samples were carried out using PHILIPS CM 200 microscope.

Raman spectroscopy and mapping of the samples was carried out using Horiba Yvon Jobin LabRAM instrument equipped with monochromatic radiation of $\lambda = 532$ nm with 5 mW power. Room temperature mapping was performed over an area » 5 μm^2 using 0.90/100x objective with spatial resolution 361 nm and depth resolution $\approx$ 1 μm. Raman mapping of the few modes to quantify the phase contribution in the nanostructures. We considered modes centered around 114 and 134 cm -1 for hexagonal and orthorhombic phases.

The magnetic measurements were carried out using QD PPMS model 6000. The samples were subjected to the zero field cooled (ZFC) and field cooled (FC) measurements under the influence of applied magnetic field at 100 Oe with the temperature varying from 2K to 400K. XANES was measured at the Beamline P64 at the PETRA III storage ring at DESY. The sample was mounted in a cryostat, and XANES-spectra were collected between 20K and room temperature (300K).

XRD

Room temperature XRD shows that the LFO-NP and LFO-NF are consisted of two pure phases, hexagonal P63cm and orthorhombic Pbnm as shown in Figure 1 (a) .Fig. 1 (b) shows the unit cell of o-LFO with space group Pbnm. The trivalent ions are located inside the corner-linked octahedra (FeO_6) with a 6-fold oxygen environment. Fig.1(c) shows unit cell of h-LFO with the space group of P63cm, where the trivalent iron ions occupy the unusual trigonal bipyramidal site (FeO_5) with a 5-fold oxygen environment. The hexagonal structure contains two crystallographically independent Lu ions Lu1 and Lu2. The Lu ions are surrounded by eight O ions. The Fe ion forms a FeO_5 trigonal bipyramid with two apical O ions, O1 and O2 ions and three in- plane O ions, one O3 and two O4 ions. The Lu and Fe ions form the triangular lattice layers, respectively. These Lu and FeO_5 trigonal bipyramid layers alternately placed along the c-axis. [2]

To obtain accurate structural parameters for our LFO-NP and LFO-NF samples, Rietveld refinements of the room temperature XRD data as shown in Figure 1 (a). The percentage composition of orthorhombic and hexagonal phases (assuming that percent contribution of each phase to total intensity is equal to their mass percent) in LFO-NP (75% -o and 25%-h) and LFO-NF (23-o and 77%-h) indicating the NF has more of hexagonal phase.
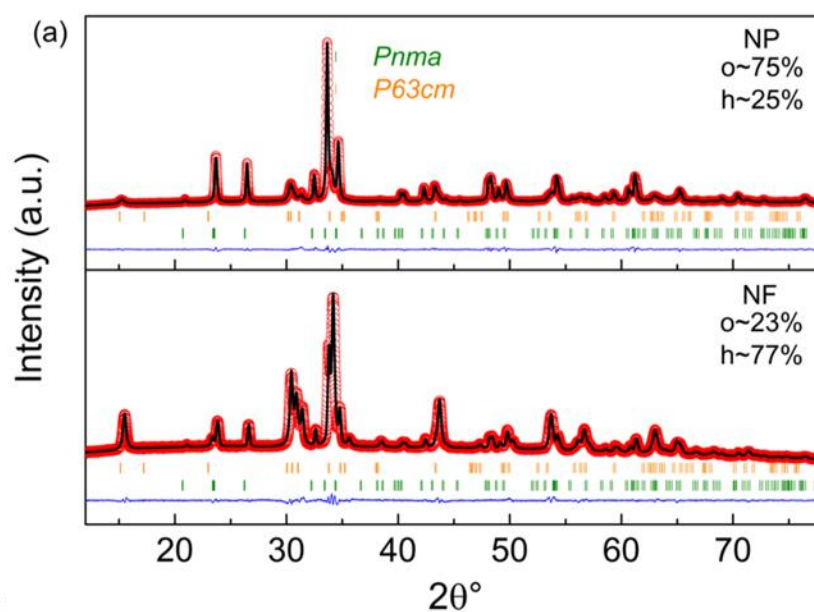
Figure S1. Refined X ray diffraction data[1] (Reproduced from Ref. 3 with permission from the Royal Society of Chemistry.)

$RFeO_3$ generally grow in orthorhombic crystal symmetry. $LuFeO_3$ is rare earth perovskite which can form orthorhombic (o) and hexagonal (h) phases. Hexagonal structure is an intermediate metastable state while growing from amorphous to orthorhombic state.[3]

Magnetism

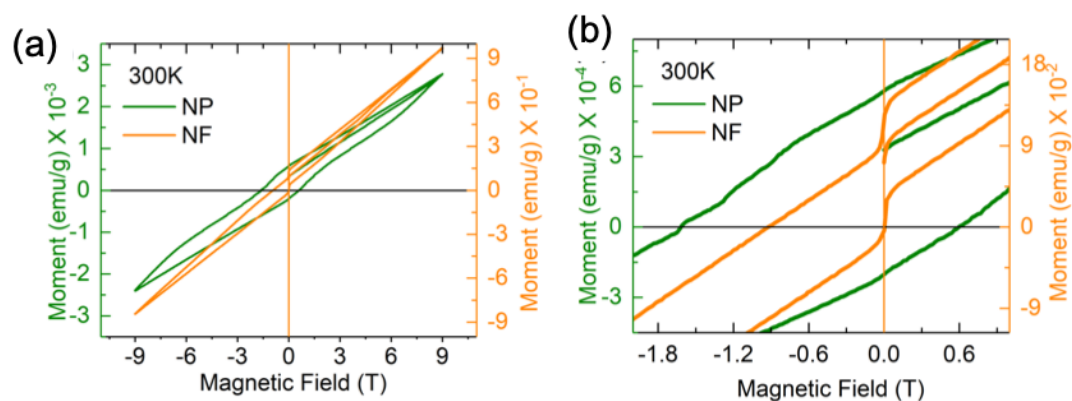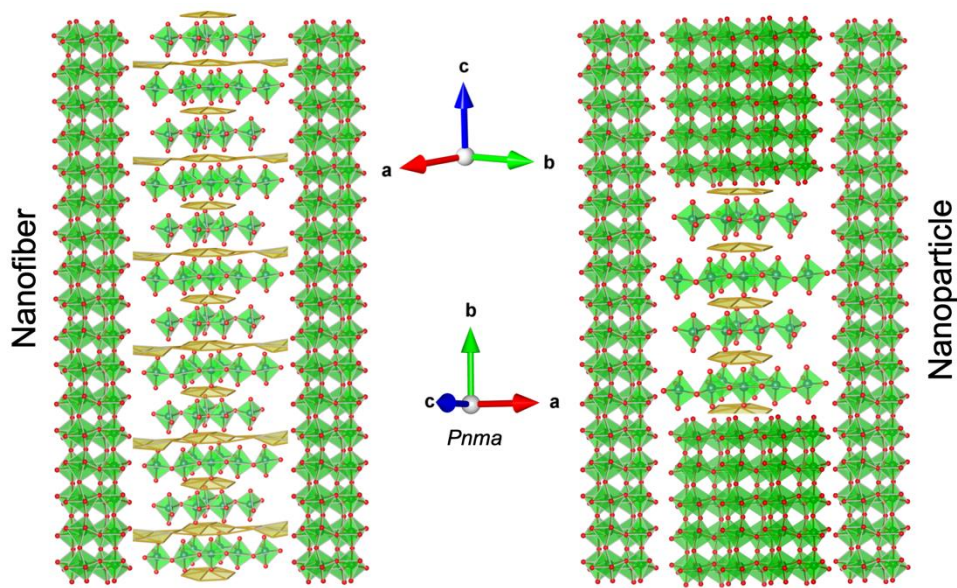The magnetic hysteresis loops were measured at 300K shown in figure 2 (a) and (b).

Figure S2. M-H loop data for NP and NF (a)300 K, (b) zoomed out view 300 K.

Scheme 1. The cross section view of the atomic arrangement showing the nature of interfaces between the nanofibre and nanoparticles.

TableS1. Calculated crystal field splitting Energy

	NPs			**NFs**		
	$t_{2g}(eV)$	$e_g(eV)$	$\Delta_o(eV)$	$t_{2g}(eV)$	$e_g(eV)$	$\Delta_o(eV)$
20	7114.91	7113.58	1.33	7115.43	7113.75	1.68
50	7114.99	7113.72	1.27	7115.45	7113.74	1.71
100	7115.45	7113.73	1.72	7115.21	7113.75	1.46
150	7115.13	7113.55	1.58	7115.34	7113.76	1.58
200	7115.21	7113.68	1.53	7115.3	7113.72	1.58
250	7115.08	7113.61	1.47	7115.1	7113.75	1.35
300	7115.07	7113.64	1.43	7114.8	7113.72	1.08

[1] S. Chaturvedi, P. Shyam, A. Apte, J. Kumar, A. Bhattacharyya, A.M. Awasthi, and S. Kulkarni, Phys. Rev. B **93**, 174117 (2016).

[2] E. Magome, C. Moriyoshi, Y. Kuroiwa, A. Masuno, and H. Inoue, Jpn. J. Appl. Phys. **49**, 09ME06 (2010).

[3] S. Chaturvedi, S.K. Singh, P. Shyam, M.M. Shirolkar, S. Krishna, R. Boomishankar, and S. Ogale, Nanoscale **10**, 21406 (2018).

[4] W. Zhu, L. Pi, S. Tan, and Y. Zhang, Appl. Phys. Lett. **100**, 052407 (2012).